


Article

An Assessment of the Role of Combined Bulk Micro- and Nano-Bubbles in Quartz Flotation

Shaoqi Zhou ^{1,2}, Yang Li ^{1,2}, Sabereh Nazari ², Xiangning Bu ^{1,2,*}, Ahmad Hassanzadeh ^{3,4,*} , Chao Ni ¹,
Yaqun He ¹ and Guangyuan Xie ^{1,2}

¹ Key Laboratory of Coal Processing and Efficient Utilization (Ministry of Education), China University of Mining and Technology, Xuzhou 221116, China; shaoqi_zhou@163.com (S.Z.); TS21040172P31@cumt.edu.cn (Y.L.); sunnichao@126.com (C.N.); yqhe@cumt.edu.cn (Y.H.); xgywl@163.com (G.X.)

² School of Chemical Engineering and Technology, China University of Mining and Technology, Xuzhou 221116, China; tbh240@cumt.edu.cn

³ Department of Geoscience and Petroleum, Faculty of Engineering, Norwegian University of Science and Technology, 7031 Trondheim, Norway

⁴ Maelgwyn Mineral Services Ltd., Ty Maelgwyn, 1A Gower Road, Cathays, Cardiff CF24 4PA, UK

* Correspondence: xiangning.bu@cumt.edu.cn (X.B.); ahmad.hassanzadeh@ntnu.no (A.H.)

Abstract: Bulk micro-nano-bubbles (BMNBs) have been proven to be effective at improving the flotation recovery and kinetics of fine-grained minerals. However, there is currently no research reported on the correlation between the properties of BMNBs and flotation performance. For this purpose, aqueous dispersions with diverse properties were created by altering preparation time (0, 1, 2, 3, 5, and 7 min), aeration rate (0, 0.5, 1, 1.5, and 2 L/min) and aging time (0, 0.5, 1, and >3 min). Micro- and nano-bubbles were characterized using focused beam reflection measurements (FBRM) and nanoparticle tracking analysis (NTA), respectively. The micro-flotation of quartz particles was performed using an XFG-cell in the presence and absence of BMNBs with Cetyltrimethylammonium bromide (CTAB) as a collector. The characterization of bubble sizes showed that the bulk micro-bubble (BMB) and bulk nanobubble (BNB) diameters ranged from 1–10 μm and 50–400 nm, respectively. It was found that the preparation parameters and aging time considerably affected the number of generated bubbles. When BNBs and BMBs coexisted, the recovery of fine quartz particles significantly improved (about 7%), while in the presence of only BNBs the promotion of flotation recovery was not significant (2%). This was mainly related to the aggregate via bridging, which was an advantage for quartz flotation. In comparison, no aggregates were detected when only nano-bubbles were present in the bulk solution.

Keywords: bulk micro-nanobubbles; bubble size and number; flotation; aggregation; quartz



Citation: Zhou, S.; Li, Y.; Nazari, S.; Bu, X.; Hassanzadeh, A.; Ni, C.; He, Y.; Xie, G. An Assessment of the Role of Combined Bulk Micro- and Nano-Bubbles in Quartz Flotation. *Minerals* **2022**, *12*, 944. <https://doi.org/10.3390/min12080944>

Academic Editor: Kevin Galvin

Received: 8 July 2022

Accepted: 24 July 2022

Published: 27 July 2022

Publisher's Note: MDPI stays neutral with regard to jurisdictional claims in published maps and institutional affiliations.



Copyright: © 2022 by the authors. Licensee MDPI, Basel, Switzerland. This article is an open access article distributed under the terms and conditions of the Creative Commons Attribution (CC BY) license (<https://creativecommons.org/licenses/by/4.0/>).

1. Introduction

BMNBs have been found to be effective in improving the flotation recovery and kinetics of coals and minerals [1–5]. A variety of acceptable bubble generation methods have been applied in the flotation process, such as ultrasonic cavitation [6–8], temperature difference [9,10], compression–decompression [11–13], and hydrodynamic cavitation techniques. Compared to the methods mentioned above, hydrodynamic cavitation has continuously been regarded as a cost-effective method for fine particle flotation [14–17]. Hydrodynamic cavitation has been found to have two modalities of use in flotation. The first approach is direct pulp treatment, i.e., three-phase cavitation (gas-liquid-solid). The other method is to treat the water/reagent solution by two-phase (gas-liquid) cavitation and then employ the BMNB-containing solution in the flotation process.

Three-phase cavitation in fine mineral flotation is thought to date back to the 1990s [14]. Zhou [14] summarized the mechanism by which cavitation bubbles promotes flotation,

which is as follows: (i) Aggregates are formed due to the bridging of microbubbles, which promotes the attachment probability between particles and conventional bubbles. (ii) Some tiny bubbles frost on the surface of hydrophobic particles (or nucleate in situ), which improves the hydrophobicity of particles. (iii) The collapse of some cavitation bubbles can clean the particle surface (e.g., removal of slime coatings, removal of oxidation films). Moreover, they believed that the gas nuclei formed in situ on the surface of particles (which can be considered as surface nanobubbles) during the cavitation process were more efficient at promoting fine-mineral separation [18–22]. Since then, Fan et al. published a series of articles on hydrodynamic cavitation to produce micro- and nano-bubbles for flotation [23–26]. They believed that the attachment of nano-bubbles on the surface of particles in the process of cavitation is the leading mechanism for promoting the separation performance of fine minerals. However, in their research, it was found to be inappropriate to use the characteristics of fine bubbles generated under two-phase conditions to explain their role in sophisticated three-phase cavitation. Additionally, there was no well-defined equipment to monitor micro- and nano-bubbles in bulk solutions neither statistically nor dynamically.

Compared with applying three-phase cavitation in flotation, the application of a micro-/nano-bubble aqueous dispersion prepared by two-phase cavitation in flotation seems to be more economical [27–29]. On the one hand, the concentration of BMNBs produced in this way is considerably higher than that of three-phase cavitation. In addition, it avoids the high wear and high energy consumption of traditional three-phase cavitation [3,30,31]. Some researchers applied the high concentration of micro-bubble-containing solutions prepared by hydrodynamic cavitation to the flotation of fine materials. The experimental results indicated that the inclusion of such bubbles could increase the flotation yield of fine minerals and dramatically improves their flotation kinetics [1,32–35]. For example, Rulyov [34] found that the treatment of micro-bubbles and glass beads mixture in the flotation reactor significantly improved the recovery of glass beads in the flotation column, which was attributed to the formation of coarse hetero-aggregates made up of multiple beads and microbubbles. Similar results were also presented in the research of Farrokhpay [35]. However, in the process of preparing micro-bubbles, bulk nano-bubbles were also produced at the same time, which was not mentioned in their research. Hence, the mechanism of these high concentration micro- and nano-bubbles in fine particle flotation is still unclear.

Recently, some researchers systematically studied the influence of operating parameters on the properties of BMNBs [36–40]. For example, Pourkarimi et al. [41] found that nanobubble diameters enlarged after increasing the dissolved air flow rate and decreased after increasing the pressure within the nano-bubble generator. Zhou [31] found that the size and number of micro- and nano-bubbles were significantly affected by the preparation parameters. However, there is no research available on the correlation between the properties of BMNBs and flotation performance in the existing literature. Thus, by examining the features of bulk micro-bubbles (BMBs) and bulk nano-bubbles (BNBs) under various operating settings and their effect on the flotation performance, it is possible to understand better the role of bubbles of various sizes in increasing the flotation performance.

In this study, the effect of the preparation parameters including preparation time, and aeration rate as well as ageing time was investigated on different scales of bubble clusters. Aside from this, the effect of combined micro- and nano-bubbles with different properties on fine quartz flotation was revealed. Finally, by examining the effect of several aqueous dispersions with varying bubble cluster compositions on flotation performance, the role of micro- and nano-bubbles in quartz flotation was discussed.

2. Methodology

2.1. Materials and Reagents

The flotation experiments were conducted on high-purity quartz samples taken from Jiangsu province, China. A laser particle size analyzer (GSL-1000, Liaoning instrument

research institute Co., Ltd., Dandong City, China) was employed to measure the particle size distribution (Figure 1). According to Figure 1, the quartz sample had a d_{50} of 15.54 μm . The X-ray diffractometer (XRD, Bruker, Bremen, Germany) revealed that quartz was the dominant component of the sample (Figure 2). Analytical grade cetyltrimethylammonium bromide (CTAB) was purchased from Sinopharm Chemical Reagent Co., Ltd, Shanghai, China. and used as a collector. Deionized water with a conductivity of 18.2 $\text{M}\Omega\cdot\text{cm}$ was utilized in all experimental works.

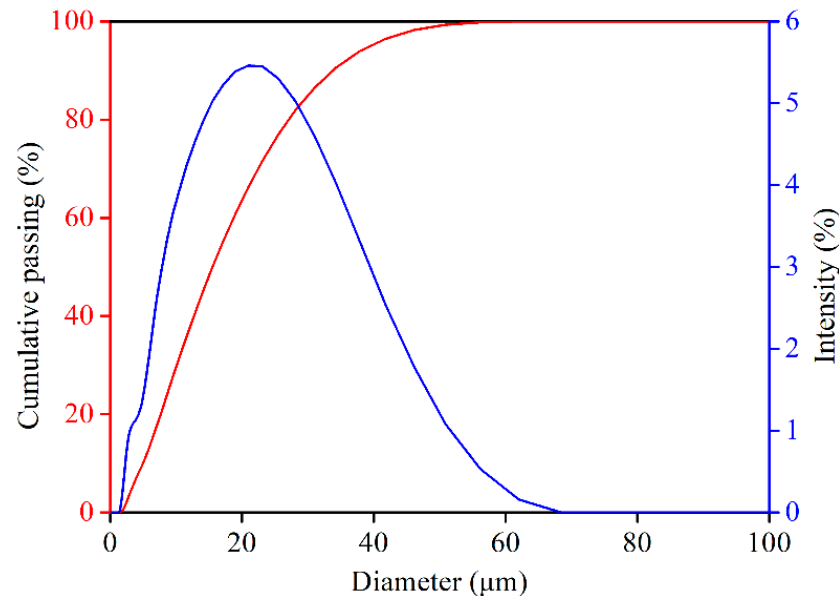


Figure 1. Particle size distribution of quartz sample.

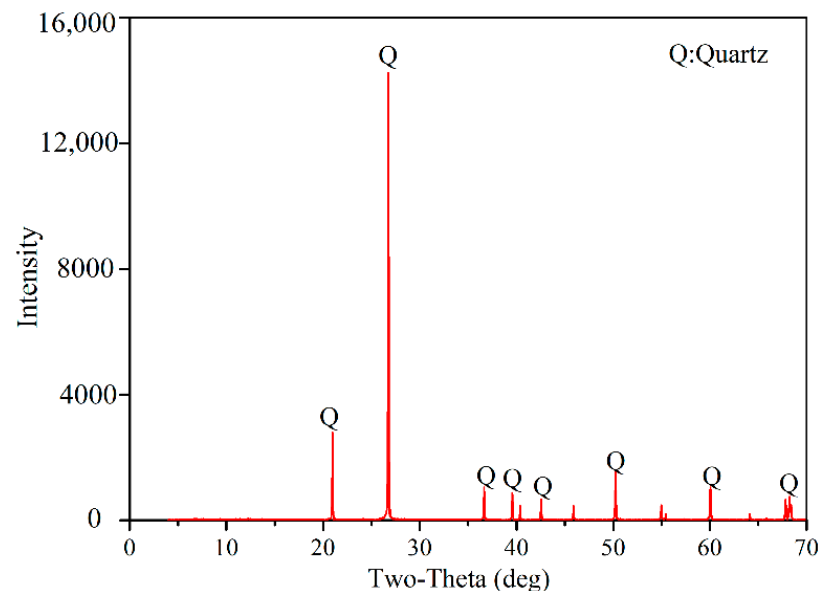


Figure 2. XRD patterns of studied quartz sample.

2.2. Preparation and Characterization of Aqueous Dispersions

A fine-bubble generator (Xiazhichun Environmental Protection Technology Co., Ltd., Kunming, China) was used to produce small size bubbles via hydrodynamic cavitation. Detailed information regarding the operating parameters and their mechanisms can be found elsewhere [32,42]. The generator works by combining and mixing water and air through a pump and venturi tube, and releasing uniform BMNBs through a fine bubble nozzle to form an “emulsion-like” gas-liquid mixture. To produce micro- and nano-bubbles,

5 L of ultrapure water was circulated into the equipment. The aqueous solutions with different properties were prepared by adjusting the preparation time (1–10 min) and aeration rates (0–2 L/min) before conducting the flotation experiments. All the tests were carried out at room temperature (25 °C).

Since it is not feasible to monitor both micro- and nano-bubbles simultaneously, two different pieces of equipment were used for their quantifications. The number, concentration, and the size distribution of bulk micro-bubbles in the solution were determined using focused beam reflectance measurement (FBRM, G400, Mettler-Toledo Ltd., Columbus, OH, USA). A Mettler-Toledo ParticleView V19 system (Mettler-Toledo Ltd., Columbus, OH, USA) was used to obtain the images of bulk micro-bubbles (BMBs) and quartz flocs. Due to the instability of these bubbles, they can only be monitored in real-time, which is the advantage of FBRM [16,36,43]. The FBRM probe was placed directly into the aqueous dispersion at a fixed angle during the test, and the bubbles flowed through the probe window and were recorded dynamically. The detailed procedure for the FBRM measurement was presented previously and detailed information in this regard can be found elsewhere [44]. To exclude the influence of micro-bubbles on test accuracy during the nano-bubble related measurements, aqueous dispersions were allowed to stand for several minutes after the preparation.

The number (concentration) and size distribution of nano-bubbles in the bulk solution were monitored using Nanoparticle Tracking Analysis (NTA, NS 300, Malvern, Malvern, PA, USA). It was equipped with a laser light source (65 mW, which was equal to 405 nm), and coupled with 20× magnification microscope and a high-speed CMOS camera. Detailed information for NTA measurements is presented elsewhere [31].

2.3. Micro-Flotation Tests

Flotation experiments were performed in an XFG-5 laboratory flotation cell (Nanchang Jianfeng Mining Machinery Manufacturing Co., Ltd., Nanchang, China). During the flotation process, the impeller speed and the aeration rate of the flotation machine were set to 1000 rpm and 40 mL/min, respectively. First, 5 g of the quartz sample was weighed and then dispersed into the flotation cell containing 20 mL of pure water. Then, the flotation machine was turned on, and the pulp was conditioned for 1 min. Later, 1×10^{-5} M CTAB was added to the flotation machine with a conditioning time of 1 min. Subsequently, 100 mL of pure water (conventional test) and the freshly made aqueous dispersion (containing BMNBs) were added to the flotation cell and stirred for 1 min (Figure 3). The floating particles were collected for 2 min. Finally, both concentrates and tailing samples were filtered and dried overnight. All tests were carried out at the natural pH of 7. The flotation mass recovery was estimated using $R = C/F$, where R (%), $C(g)$, and $F(g)$ represent concentrate yield, concentrate and tailings weights, respectively.

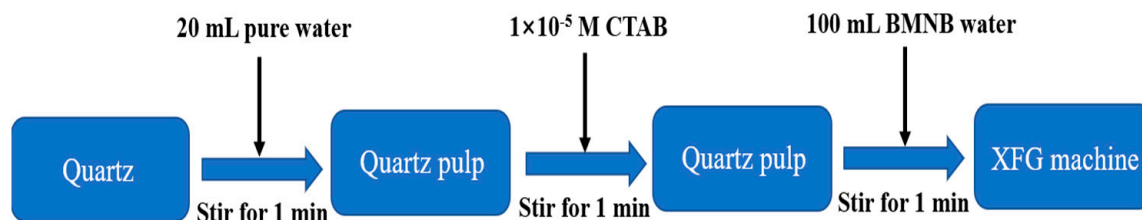


Figure 3. The step-wised experimental procedure.

3. Results and Discussions

3.1. Characteristics of BMNB

3.1.1. Effect of Aging Time

Figure 4 depicts the qualitative observation of produced aqueous solutions and bubble size measurements as a function of ageing time. It is worth noting that before preparing the dispersion, the aqueous solution was obviously clear. It turned milky immediately after preparing the solution at ageing time = 0 (Figure 4a). At this time, the aqueous dispersion

contained both micro- and nano-bubbles with a high concentration. As the ageing time increased up to 1 min, the bottom layer of the aqueous dispersion gradually became clear, while the upper layer remained milky white (Figure 4b,c). As can be seen (Figure 4d), by increase the ageing time from 3 to 10 min, the solution's milky white color progressively vanished. Therefore, the aqueous dispersion remained clear after >3 min of ageing time due to the low longevity of micro-bubbles in bulk solutions. Indeed, the existence of a high concentration of bulk micro-bubbles largely contributed to the milky white color of the aqueous dispersion. With the increase in ageing time, micron- bubbles gradually moved to the surface and burst due to their low stability, rendering the solution transparent. The same phenomenon was observed in the study reported by Nazari and Hassanzadeh [1,45]. However, bulk nano-bubbles remained in the bulk solution due to their high stability and longevity [46,47]. The number of bulk micro-bubbles as a function of ageing time is shown in Table 1. As can be seen, the concentration of these bubbles decreases as time passed and they disappeared after 3 min of ageing.

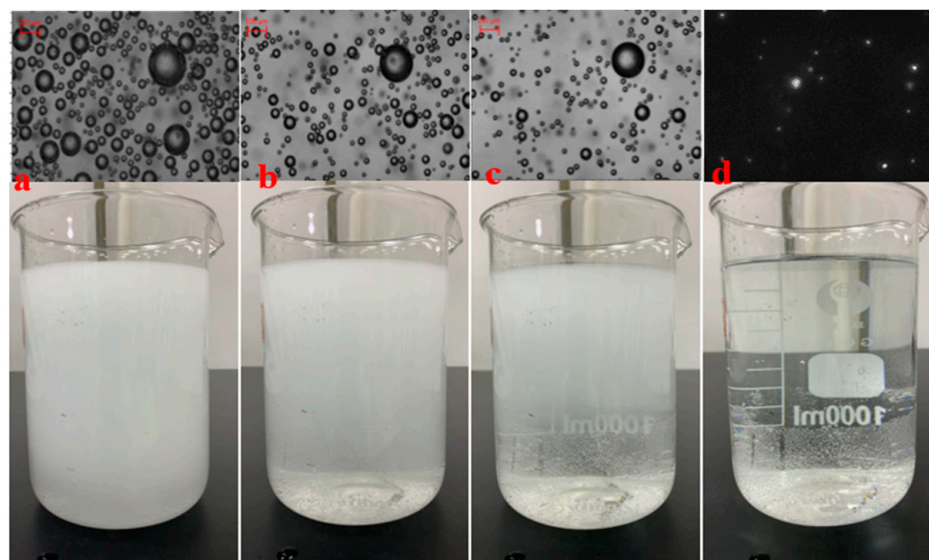


Figure 4. Variation of aqueous dispersion as a function of ageing time, at preparation time of 2 min, and aeration rate of 0.5 L/min (aging time (a): 0 min, (b): 0.5 min, (c): 1 min, and (d): >3 min).

Table 1. Variation of number of micro-bubbles with ageing time (when the preparation time = 2 min, and aeration rate = 0.5 L/min).

Bubble Size (μm)	Ageing Time (min)			
	0	0.5	1	>3
1–10	11,424	8845	5236	0
10–100	3760	2126	1509	0

3.1.2. Number of BMNBs under Different Operating Parameters

Figure 5a,b show the concentration of BNBs as a function of preparation time and aeration rate, respectively. When the aeration rate was constant, the concentration of nano-bubbles enhanced with an increased preparation time. Interestingly, it was observed that natural gas nuclei with a concentration of about 7×10^6 bubble/mL existed in pure water without any treatment. When the equipment operated from 1 min to 7 min, the nano-bubble concentration increased from 8.87×10^7 to 3.10×10^8 bubble/mL. This is because cavitation behavior continued to occur, and nano-bubbles continued to be generated during equipment operation, causing the concentration of BNBs to increase constantly. Compared with the preparation time, the aeration rate had a negligible effect on the concentration of BNBs. When the preparation time was 2 min, with the increase in the aeration rate up to 2 L/min, the concentration of BNBs initially increased, peaking

at 0.5 L/min (1.92×10^8 bubble/mL), and then decreased. A modest aeration rate may increase bubble formation, while excessive aeration can reduce cavitation intensity. The cavitation nucleation behavior greatly influences the concentration of bulk nano-bubbles. The cavitation behavior is affected by the aeration rates and preparation time. Compared to the no aeration condition, an increase in the aeration rate may reduce the pressure at the venturi throat (the pressure difference between the venturi throat and the inlet). As is known, the cavitation intensity in the venturi tube is positively correlated with the pressure difference between the throat and inlet fluid. Therefore, such an increase leads to a reduction in cavitation intensity [1], which is considerably small at a low aeration rate compared with that without aeration.

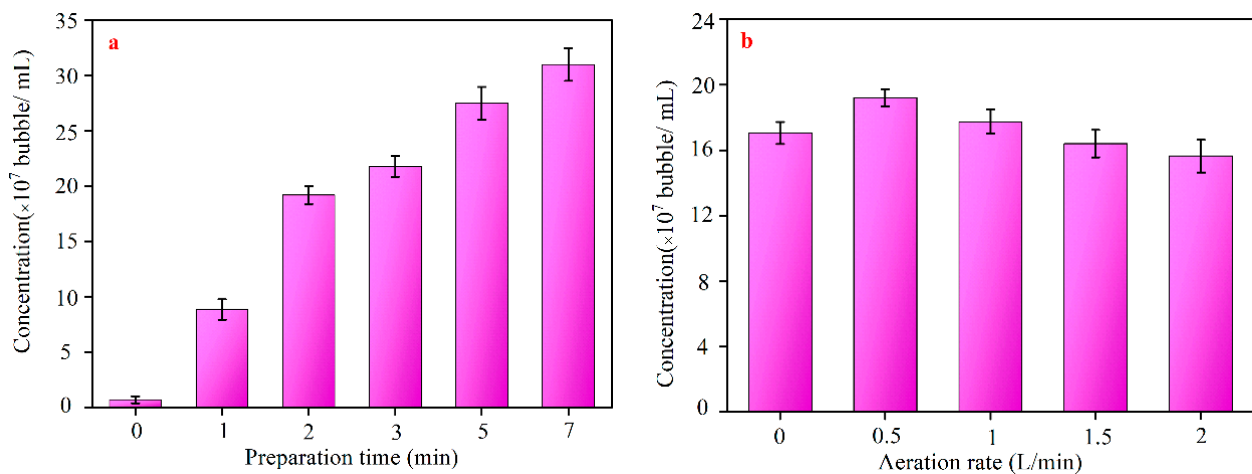


Figure 5. Concentration of bulk nanobubbles prepared as a function of (a) preparation time at an aeration rate of 0.5 L/min, and (b) aeration rate at preparation time of 2 min.

Figure 6 illustrates the number of BMBs with various scales prepared with different preparation times. The number of bubbles with a diameter of 1–10 μm (about 10,000) was always dominant regardless of the preparation time. The number of bubbles with a diameter of 10–100 μm was approximately 3700 under the optimal preparation conditions. When the aeration rate was set to 0.5 L/min, increasing the preparation time from 1 to 7 min enhanced the number of bubbles with a diameter of 1–10 μm and 10–100 μm first, reaching a maximum at 2 min, and then reduced. This is because BMBs follow the process of generation, coalescence, and rupture during the operation of the equipment; therefore, the number of bubbles rapidly increased and decreased.

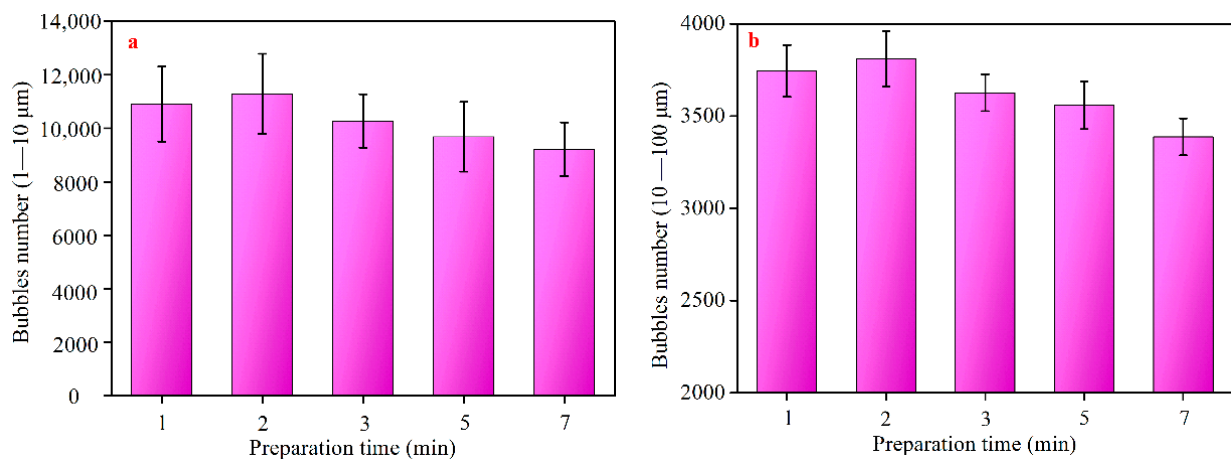


Figure 6. Number of bulk microbubbles prepared at different times: (a) 1–10 μm , and (b) 10–100 μm at aeration rate of 0.5 L/min.

Figure 7 displays the variation in the number of bulk micro-bubbles by categorizing them into two ranges of 1–10 μm and 10–100 μm . Similarly to Figure 6, bubbles with a diameter of 1–10 μm continued to prevail. As the aeration rate rose from 0 L/min to 2 L/min, the number of bubbles with a diameter of 1–10 μm and 10–100 μm also first increased and then decreased. The maximum number of bubbles was obtained at the aeration rate of 0.5 L/min for both size ranges. As the aeration rate further increased, bubble coalescence occurred and the number of bubbles decreased. This is also the reason for the change in the number of nano-bubbles. Additionally, this was also found in previous work reported by Hassanzadeh et al. [48].

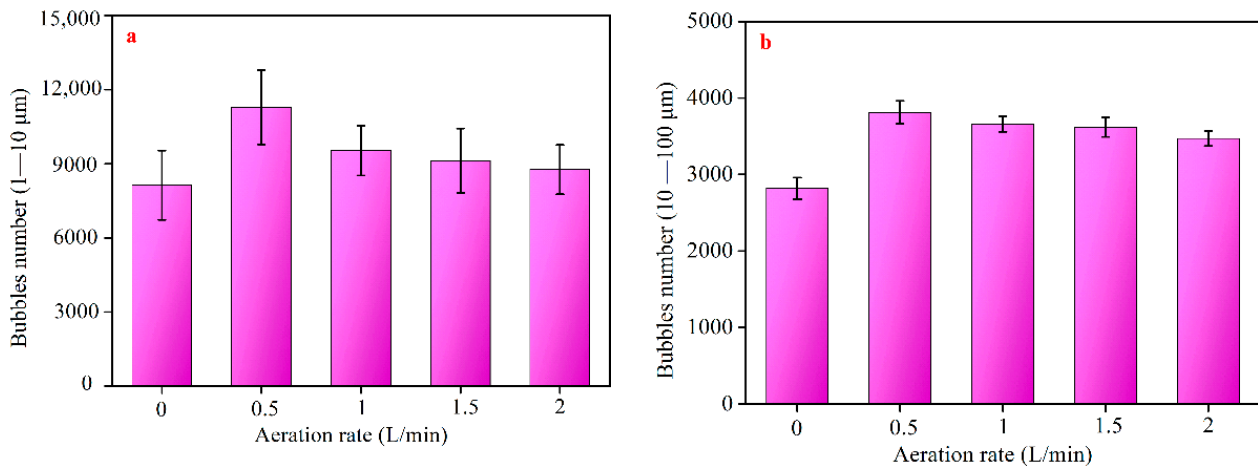


Figure 7. Number of micro-bubbles prepared at different aeration rates categorized as (a) 1–10 μm and (b) 10–100 μm when the preparation time equaled 2 min.

3.1.3. Size Distribution of BMNBs under Different Operating Parameters

As illustrated in Figure 8a,b, the operation parameters (preparation time and aeration rate) used in this investigation had no discernible effect on the size distribution of bulk micro-bubbles. Under all these conditions, the size of BMBs was between 1–100 μm , and their size distribution presented a single peak located at about 3–4 μm . The results for the bubble size distribution were consistent with those of the bubble numbers in the preceding section. In comparison with the bulk micro-bubbles, the operational parameters affected BNBs' size distribution. The size distribution of BNBs was generally between 50 and 400 nm (Figure 9a,b). Under various preparation conditions, the size distribution of nano-bubbles varied by less than 100 nm.

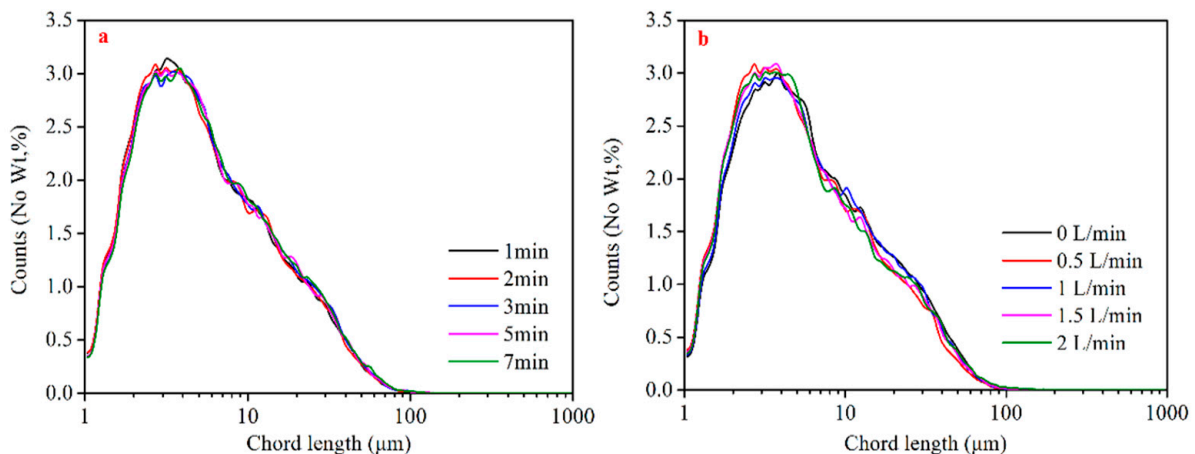


Figure 8. Size distribution of BMBs prepared under different conditions: (a) 0.5 L/min aeration rate, (b) 2 min preparation time.

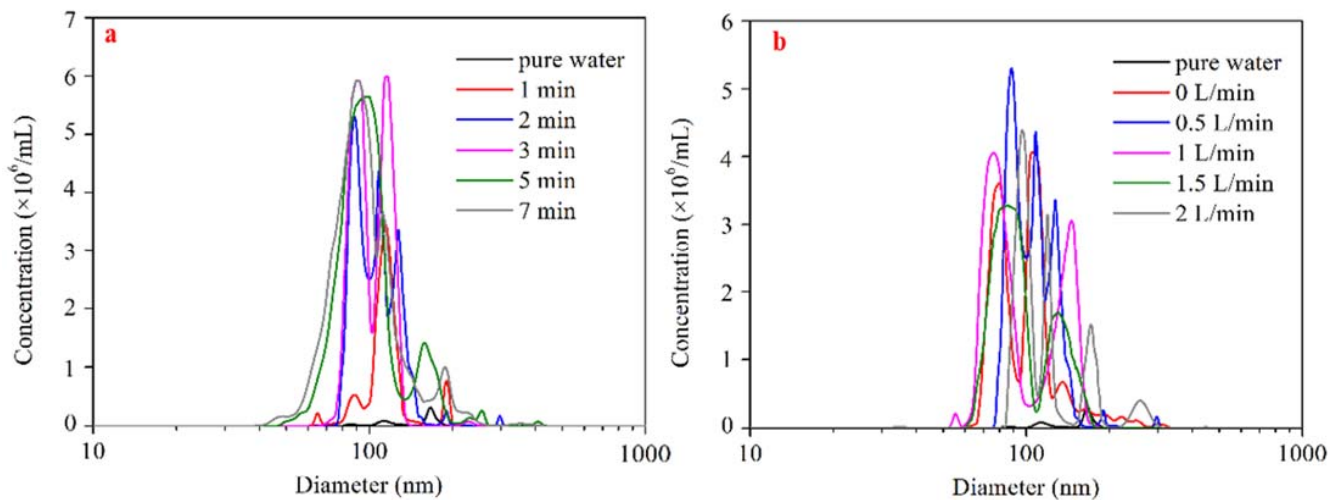


Figure 9. Size distribution and concentration of BNBs as a function of (a) preparation time at constant aeration rate of 0.5 L/min and (b) aeration rate at a stationary 2 min of preparation time.

3.2. Flotation Results

3.2.1. Effect of Ageing Time of Micro-/Nano-Bubble Water on Flotation Performance

Figure 10 shows the quartz flotation recovery as a function of ageing time. As evidenced, flotation recovery gradually reduced as the BMNBs water aged, but it was always greater than in the absence of BMNBs in the system. Specifically, when fresh aqueous dispersion (i.e., ageing time of 0 min) was used in the flotation, the recovery of froth products was about 79%. The recovery increased by 7% compared to conventional flotation (about 72%). When the ageing time was 0.5 min, the flotation recovery was about 76%. After that, by prolonging the ageing time to 5 and 10 min, the flotation recovery was maintained at approximately 73%. At this time, compared with the results of a conventional flotation test, recovery increased by only about 2%. In other words, compared to the conventional conditions, due to an increase in the ageing time, the impact of BMNBs on the flotation performance decreased gradually.

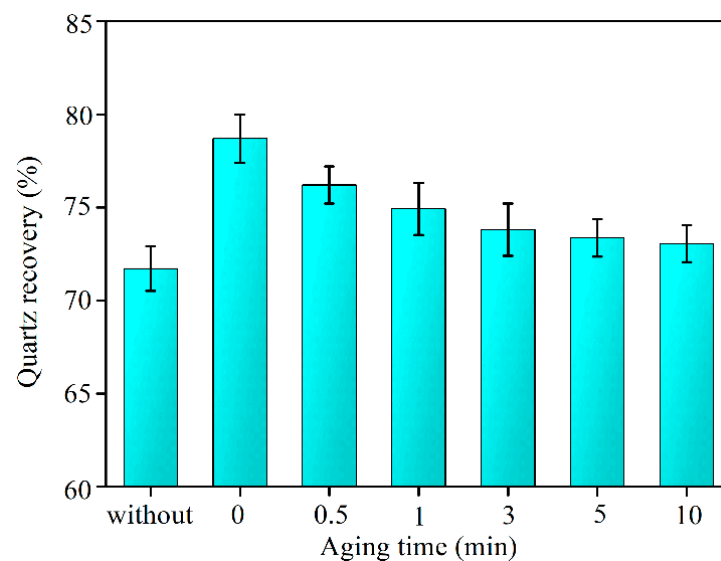


Figure 10. Flotation recovery of quartz varies with the ageing time of aqueous dispersion containing BMNBs at preparation time of 2 min and aeration rate of 0.5 L/min.

The linear relationship between flotation recovery (x) and the number of BMBs (y) during ageing is shown in Figure 11. Due to the stability of BNBs, we assumed that the number of BNBs would not change significantly during the ageing time. It can be seen

from Figure 11 that there was a robust linear relationship ($R^2 = 0.9838$) between the number of BMBs and flotation recovery. With increasing ageing time, the micron-scale bubbles in an aqueous dispersion gradually dissipated, thereby reducing flotation recovery. When the ageing time exceeded 5 min, BMBs virtually vanished, and only BNBs remained in the aqueous dispersion. This further shows that the presence of BMBs within BMNBs dispersions is critical in promoting flotation performance.

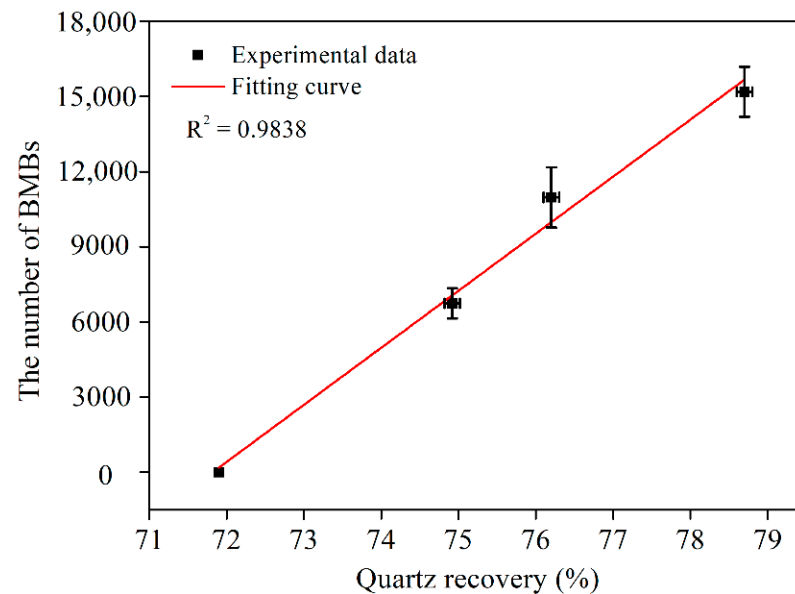


Figure 11. Number of BMBs (>1 μm) as a function of flotation recovery (under various aging times).

3.2.2. Effect of Preparation Conditions of BMNBs Water on Flotation Performance

The flotation recovery is plotted as a function of the aeration rate in Figure 12. An increase in the aeration rate from 0 to 2 L/min resulted in an increase in flotation recovery followed by a drop. When BMNBs water was created using a variety of aeration rates, the difference between the highest flotation recovery (78%, aqueous dispersion prepared with 0.5 L/min) and the lowest flotation recovery (75%, corresponded solution at 0 L/min) was less than 3%. Most notably, the change in the flotation recovery had the same trend as that of BMBs. This further showed that the flotation recovery was sensitive to the number of BMBs.

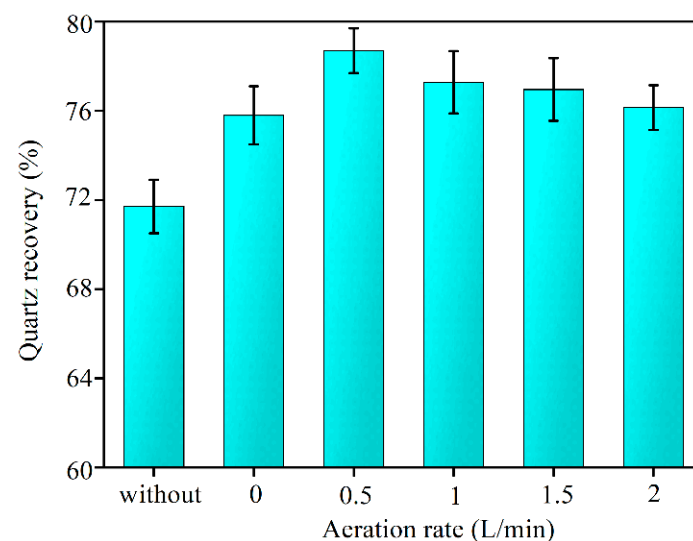


Figure 12. Effect of BMNBs water prepared by different aeration rates on flotation recovery (preparation time 2 min).

Similarly, the linear relationship between the number of bubbles (y) and the flotation recovery (x) under different aeration rates was statistically analyzed (Figure 13). There was a strong correlation between the number of BMBs and flotation recovery ($R^2 = 0.9605$); however, the correlation between the number of BNBs and flotation recovery was relatively low ($R^2 = 0.6849$). Hence, we believe that the number of BMBs plays a leading role compared to BNBs.

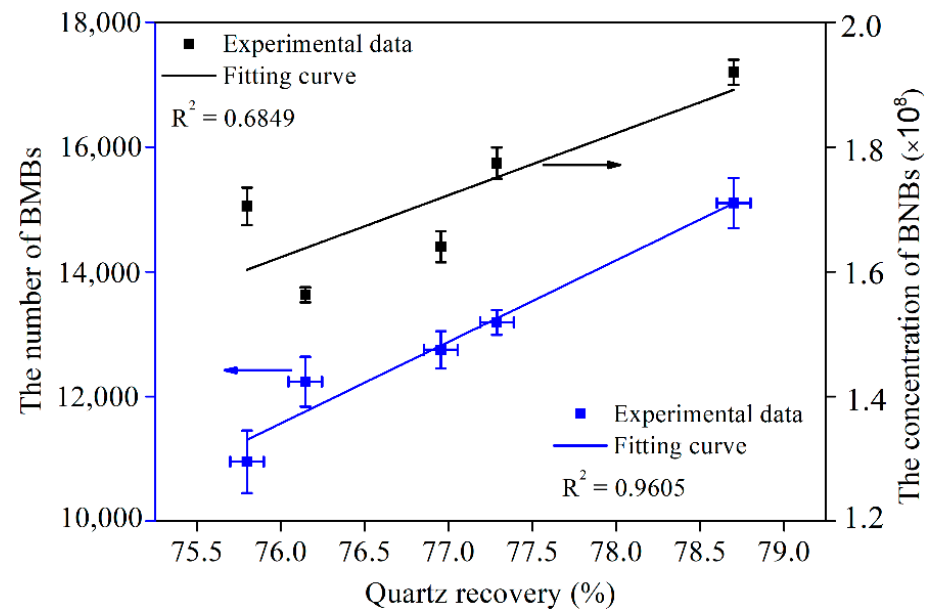


Figure 13. Number of BMBs ($>1 \mu\text{m}$) and concentration of BNBs as functions of flotation recovery (under different aeration rates).

Figure 14 illustrates the flotation recovery as a function of the time required for the preparation of BMNBs water. The flotation recovery of quartz increased with the increase in preparation time of BMNBs water. Without BMNBs (i.e., preparation time is 0 min), the flotation recovery of quartz was about 72%. When BMNBs water with a preparation time of 1 min was used for flotation, the quartz recovery was about 77%, increasing by nearly 5%. As the preparation time of BMNBs water increased from 1 min to 7 min, the recovery of quartz increased from about 77% to 82%. However, when the preparation time of BMNBs water was less than 5 min, the improvement in quartz recovery was relatively slow. When the preparation time increased to 7 min, a significant increase in recovery occurred. Although flotation recovery rose monotonically as the preparation time for BMNBs increased, the reason for this result is complex and not straightforward. As the preparation time for BMNBs water increased, both the number of micro- and nano-bubbles changed. Moreover, the temperature of BMNBs water increased markedly as the preparation time increased.

The temperature variation of aqueous dispersion with time and the results of conventional flotation at different temperatures are shown in Figure 15. When the preparation time increased from 0 min to 7 min, the temperature of the aqueous dispersion increased from 20 °C to 27 °C, and the flotation recovery increased from about 72% to about 76%. It can be seen that the rise in the aqueous dispersion temperature may have caused a large portion of the increase in flotation recovery with preparation time. This result is consistent with the results reported in another research study [49].

Compared to the influence of ageing time and aeration, the impact of preparation time for aqueous dispersions containing BMNBs on flotation performance was relatively complex. When the aeration rate remained constant, with the increase in preparation time and the number of bubbles at different scales, the temperature of the solution also changed significantly. The number of BMBs first increased and then decreased, but the number of BNBs and the aqueous dispersion temperature showed an increasing trend. Therefore, it is

difficult to analyze the relationship between the number of bubbles and flotation recovery. According to the flotation results from Figures 10 and 12, reducing the BMBs' number can weaken the improvement of flotation. However, the flotation recovery increased with the increase in preparation time due to the higher number of BNBs and the increase in the temperature of the aqueous dispersion (Figure 15). This further shows that the effect of BNBs was not significant under the experimental conditions.

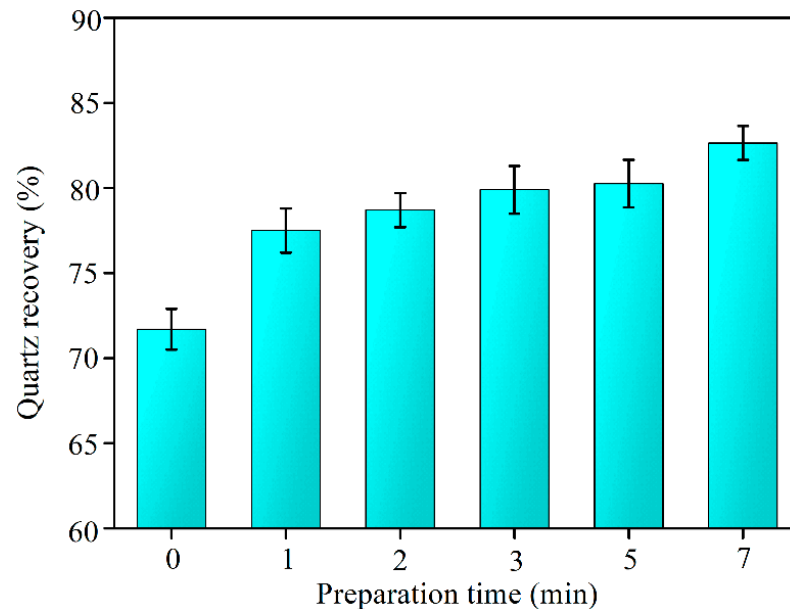


Figure 14. Effect of preparation time of BMNBs water on quartz recovery (aeration rate 0.5 L/min).

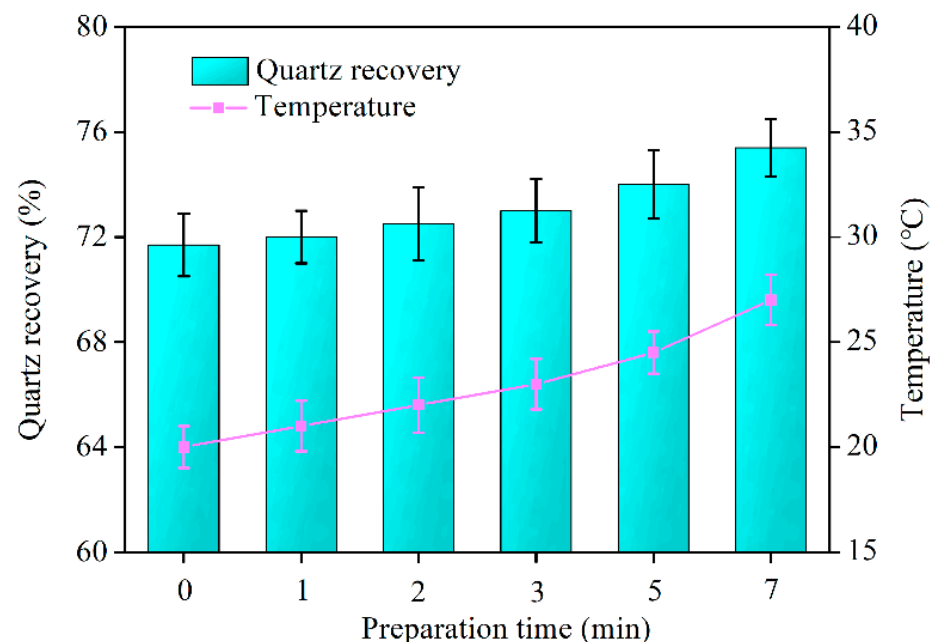


Figure 15. Effect of water temperature on flotation performance.

3.3. Discussions

As indicated previously, the dominant bubble groups in BMNBs water are bubbles with a diameter of 1–10 μm and 50–400 nm. The composition of the BMNBs groups, such as bubble number and size distribution, are affected significantly by the preparation conditions and ageing time. The number of bubbles is more sensitive to operating parameters than bubble size. For example, the concentration of BNBs changed significantly with the

change in preparation time and aeration rate, with a maximum increase of 400%. The size distribution of BMBs scarcely changed when operational parameters were changed; only the size of BNBs changed, but the variation range was less than 100 nm, and the distribution range of BNBs was relatively concentrated. Thus, the variation in flotation results under various conditions was primarily due to variations in the number of bubbles at various scales.

To further investigate the influence of BMBs and BNBs on quartz particle aggregation, the aggregation of quartz particles in the presence of BMBs and BNBs (ageing time 0 min) and only BNBs (ageing time > 3 min) was observed. As can be seen from Figure 16, when BMBs and BNBs existed simultaneously (i.e., the ageing time was 0), many flocs bridged by micro-bubbles appeared in the pulp (Figure 16c). However, no flocs (Figure 16d) were found in the presence of BNB alone (i.e., the ageing time > 3 min). Although the number of BNBs was much higher than that of BMBs, its effect on inducing particle aggregation was relatively weak. This is because, on the micro-scale, the probability of collision between particles and bubbles increases with a decrease in the bubble size [50]. BMBs can easily collide and adhere with quartz particles to form flocs. Additionally, the apparent size of flocs is much higher than that of quartz ore; it is easier to collide and adhere with conventional flotation bubbles [51]. This is beneficial for increased flotation recovery. These findings confirm the principles of the combined micro-flotation process presented in the paper of Rulyov [34]. However, no investigations were conducted to demonstrate that this rule holds for nano-bubbles because inertia no longer significantly affects the motion of nano-bubbles and Brownian motion takes over [52]. Even if BNBs can successfully collide with mineral particles, their attachment is dependent on the mineral's hydrophobicity; thus, a sufficiently hydrophobic surface is required. Additionally, because BNBs are so small, even if many of them attach to the mineral surface, their regions will be weak. This may also explain why BNBs do not greatly promote flotation performance under experimental settings.

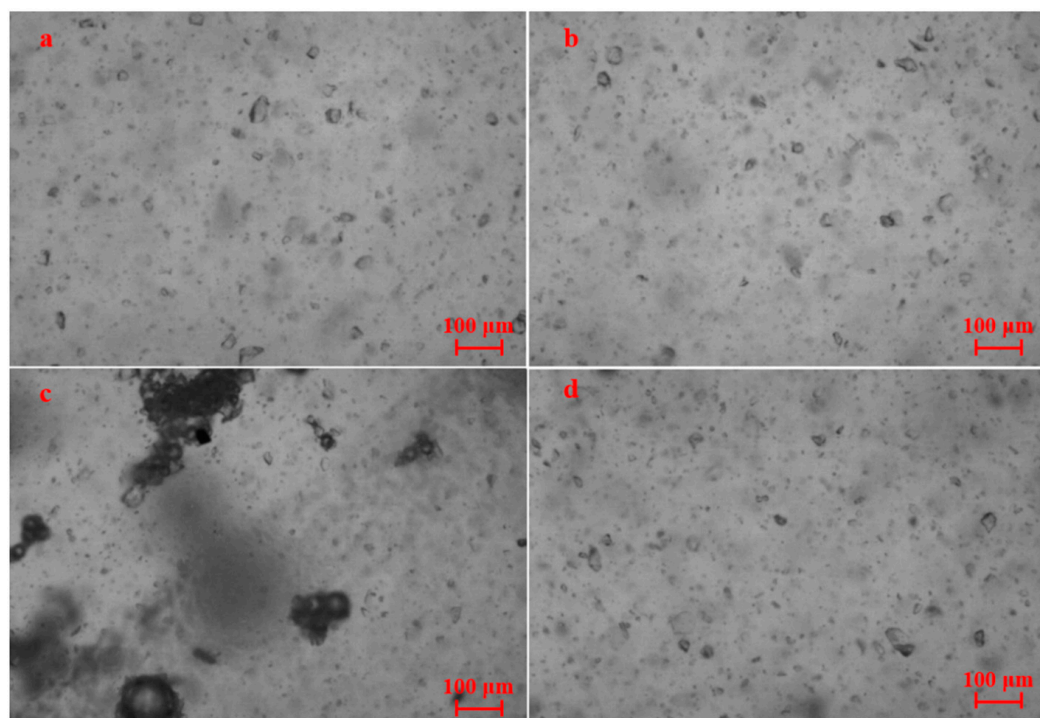


Figure 16. Quartz aggregates under different conditions conditions (a) raw quartz ore; (b) quartz + 1×10^{-5} M CTAB; (c) quartz + 1×10^{-5} M CTAB + BMNBs with the ageing time of 0 min; (d) quartz + 1×10^{-5} M CTAB + BMNBs with ageing time > 3 min).

4. Conclusions

The present work initially investigated the synergetic effect of bulk micro-nano-bubbles on the flotation of quartz particles. Bubble size distribution and stability for both ranges were studied using FBRM and NTA. The results revealed that the preparation parameters and aging times had a considerable impact on the number of bubbles with different sizes. The bubble size ranges of the BMNB-containing dispersion were obtained between 0 and 100 microns. Bubbles with diameters of 1–10 nm and 50–200 nm were predominant among them. With an increase in the aging time, the micro-bubbles were essentially vanished after 3 min, leaving just BNBs in the solution.

It was demonstrated that in the presence of BMNBs, the improvement of flotation recovery was affected by the synergistic effect of bubbles with various scales in the aqueous dispersion. Compared with the size distribution of BMNBs, the flotation recovery was more sensitive to the variation in the number of bubbles on different scales. The flotation tests with BMBs and BNBs showed higher recoveries in comparison with those tested in the absence of BMBs. When both micro and nano-bubbles existed at the same time, the yield of fine-grained quartz increased by about 7%, while when there were only BNBs, the promotion of flotation recovery was about 2%. Thus, the existence of BMBs was a key factor in promoting the flotation of fine quartz particles. As a result of forming these bubble sizes simultaneously, many flocs were bridged by BMBs in the pulp.

Author Contributions: S.Z.: methodology, validation, formal analysis, investigation, writing—original draft; Y.L.: formal analysis and investigation; S.N.: writing—review and editing, methodology, and validation; X.B.: conceptualization, data curation, writing—review and editing, visualization, project administration, funding acquisition; A.H.: writing—data analysis, review and editing; C.N.: visualization; Y.H.: investigation, review and editing; G.X.: funding acquisition, project administration. All authors have read and agreed to the published version of the manuscript.

Funding: The authors gratefully acknowledge financial support from the Fundamental Research Funds for the Central Universities, China (No. 2019XKQYMS18) and the National Natural Science Foundation of China (Grant No. 51904296 and 52074288).

Data Availability Statement: Not applicable.

Conflicts of Interest: The authors declare no conflict of interest.

References

1. Nazari, S.; Hassanzadeh, A. The effect of reagent type on generating bulk sub-micron (nano) bubbles and flotation kinetics of coarse-sized quartz particles. *Powder Technol.* **2020**, *374*, 160–171. [[CrossRef](#)]
2. Azevedo, A.; Oliveira, H.; Rubio, J. Bulk nanobubbles in the mineral and environmental areas: Updating research and applications. *Adv. Colloid Interface Sci.* **2019**, *271*, 101992. [[CrossRef](#)]
3. Calgaroto, S.; Wilberg, K.Q.; Rubio, J. On the nanobubbles interfacial properties and future applications in flotation. *Miner. Eng.* **2014**, *60*, 33–40. [[CrossRef](#)]
4. Calgaroto, S.; Azevedo, A.; Rubio, J. Flotation of quartz particles assisted by nanobubbles. *Int. J. Miner. Process.* **2015**, *137*, 64–70. [[CrossRef](#)]
5. Kruszelnicki, M.; Hassanzadeh, A.; Legawiec, K.J.; Polowczyk, I.; Kowalczyk, P.B. Effect of ultrasound pre-treatment on carbonaceous copper-bearing shale flotation. *Ultrason. Sonochem.* **2022**, *84*, 105962. [[CrossRef](#)]
6. Chen, Y.; Bu, X.; Truong, V.N.; Peng, Y.; Xie, G.y. Study on the effects of pre-conditioning time on the floatability of molybdenite from the perspective of cavitation threshold. *Miner. Eng.* **2019**, *141*, 105845. [[CrossRef](#)]
7. Chen, Y.; Xie, G.; Chang, J.; Grundy, J.; Liu, Q. A study of coal aggregation by standing-wave ultrasound. *Fuel* **2019**, *248*, 38–46. [[CrossRef](#)]
8. Chen, Y.; Truong, V.; Bu, X.; Xie, G. A review of effects and applications of ultrasound in mineral flotation. *Ultrason. Sonochem.* **2019**, *60*, 104739. [[CrossRef](#)]
9. Zhang, F.; Xing, Y.; Chang, G.; Yang, Z.; Cao, Y.; Gui, X. Enhanced lignite flotation using interfacial nanobubbles based on temperature difference method. *Fuel* **2021**, *293*, 120313. [[CrossRef](#)]
10. Li, C.; Xu, M.; Xing, Y.; Zhang, H.; Peuker, U.A. Efficient separation of fine coal assisted by surface nanobubbles. *Sep. Purif. Technol.* **2020**, *249*, 117163. [[CrossRef](#)]
11. Wang, Y.; Pan, Z.; Jiao, F.; Qin, W. Understanding bubble growth process under decompression and its effects on the flotation phenomena. *Miner. Eng.* **2020**, *145*, 106066. [[CrossRef](#)]

12. Wang, Y.; Pan, Z.; Luo, X.; Qin, W.; Jiao, F. Effect of nanobubbles on adsorption of sodium oleate on calcite surface. *Miner. Eng.* **2019**, *133*, 127–137. [[CrossRef](#)]
13. Xu, M.; Li, C.; Zhang, H.; Kupka, N.; Peuker, U.A.; Rudolph, M. A contribution to exploring the importance of surface air nucleation in froth flotation—The effects of dissolved air on graphite flotation. *Colloids Surf. A Physicochem. Eng. Asp.* **2022**, *633*, 127866. [[CrossRef](#)]
14. Zhou, Z.A.; Xu, Z.; Finch, J.A.; Hu, H.; Rao, S.R. Role of hydrodynamic cavitation in fine particle flotation. *Int. J. Miner. Process.* **1997**, *51*, 139–149. [[CrossRef](#)]
15. Li, H. Role of Hydrodynamic Cavitation in Fine Particle Flotation. Master's Thesis, University of Alberta, Edmonton, AB, Canada, 2014.
16. Zhou, S.; Wang, X.; Bu, X.; Wang, M.; An, B.; Shao, H.; Ni, C.; Peng, Y.; Xie, G. A novel flotation technique combining carrier flotation and cavitation bubbles to enhance separation efficiency of ultra-fine particles. *Ultrason. Sonochem.* **2020**, *64*, 105005. [[CrossRef](#)]
17. Nazari, S.; Hassanzadeh, A.; He, Y.; Khoshdast, H.; Kowalczyk, P.B. Recent Developments in Generation, Detection and Application of Nanobubbles in Flotation. *Minerals* **2022**, *12*, 462. [[CrossRef](#)]
18. Zhou, Z.A.; Xu, Z.; Finch, J.A.; Masliyah, J.H.; Chow, R.S. On the role of cavitation in particle collection in flotation—A critical review. II. *Miner. Eng.* **2009**, *22*, 419–433. [[CrossRef](#)]
19. Zhou, Z.A.; Xu, Z.; Finch, J.A. On the role of cavitation in particle collection during flotation—A critical review. *Miner. Eng.* **1994**, *7*, 1073–1084. [[CrossRef](#)]
20. Zhou, Z.A.; Xu, Z.; Finch, J.A. Effect of surface properties of fine particles on dynamic bubble formation in gas-supersaturated systems. *Ind. Eng. Chem. Res.* **1998**, *37*, 1998–2004. [[CrossRef](#)]
21. Zhou, Z.A.; Xu, Z.; Finch, J.A.; Liu, Q. Effect of gas nuclei on the filtration of fine particles with different surface properties. *Colloids Surf. A Physicochem. Eng. Asp.* **1996**, *113*, 67–77. [[CrossRef](#)]
22. Zhou, Z. Comment on Aqueous dispersions of nanobubbles: Generation, properties and features by A. Azevedo, R. Etchepare, S. Calgaroto, J. Rubio [*Miner. Eng.* 94 (2016) 2Y 37]. *Miner. Eng.* **2018**, *117*, 117–120. [[CrossRef](#)]
23. Fan, M.; Tao, D.; Honaker, R.; Luo, Z. Nanobubble generation and its applications in froth flotation (part IV): Mechanical cells and specially designed column flotation of coal. *Min. Sci. Technol.* **2010**, *20*, 641–671. [[CrossRef](#)]
24. Maoming, F.; Daniel, T.; Honaker, R.; Zhenfu, L. Nanobubble generation and its applications in froth flotation (part III): Specially designed laboratory scale column flotation of phosphate. *Min. Sci. Technol.* **2010**, *20*, 317–338.
25. Maoming, F.; Daniel, T.; Honaker, R.; Zhenfu, L. Nanobubble generation and its application in froth flotation (part I): Nanobubble generation and its effects on properties of microbubble and millimeter scale bubble solutions. *Min. Sci. Technol.* **2010**, *20*, 1–19.
26. Fan, M.; Zhao, Y.; Tao, D. Fundamental studies of nanobubble generation and applications in flotation. In *Separation Technologies for Minerals, Coal and Earth Resources*; Society for Mining, Metallurgy & Exploration (SME): Englewood, CO, USA, 2012; pp. 459–469.
27. Nazari, S.; Shafaei, S.Z.; Gharabaghi, M.; Ahmadi, R.; Shahbazi, B.; Maoming, F. Effects of nanobubble and hydrodynamic parameters on coarse quartz flotation. *Int. J. Min. Sci. Technol.* **2019**, *29*, 289–295. [[CrossRef](#)]
28. Zhou, W.; Liu, K.; Wang, L.; Zhou, B.; Niu, J.; Ou, L. The role of bulk micro-nanobubbles in reagent desorption and potential implication in flotation separation of highly hydrophobized minerals. *Ultrason. Sonochem.* **2020**, *64*, 104996. [[CrossRef](#)]
29. Zhou, W.; Liu, L.; Zhou, B.; Weng, L.; Li, J.; Liu, C.; Yang, S.; Wu, C.; Liu, K. Electrokinetic potential reduction of fine particles induced by gas nucleation. *Ultrason. Sonochem.* **2020**, *67*, 105167. [[CrossRef](#)]
30. Zhou, W.; Niu, J.; Xiao, W.; Ou, L. Adsorption of bulk nanobubbles on the chemically surface-modified muscovite minerals. *Ultrason. Sonochem.* **2019**, *51*, 31–39. [[CrossRef](#)]
31. Zhou, S.; Nazari, S.; Hassanzadeh, A.; Bu, X.; Ni, C.; Peng, Y.; Xie, G.; He, Y. The effect of preparation time and aeration rate on the properties of bulk micro-nanobubble water using hydrodynamic cavitation. *Ultrason. Sonochem.* **2022**, *84*, 105965. [[CrossRef](#)]
32. Zhang, Z.; Ren, L.; Zhang, Y. Role of nanobubbles in the flotation of fine rutile particles. *Miner. Eng.* **2021**, *172*, 107140. [[CrossRef](#)]
33. Rulyov, N. Combined microflotation of fine minerals: Theory and experiment. *Miner. Process. Extr. Metall.* **2016**, *125*, 81–85. [[CrossRef](#)]
34. Rulyov, N.; Sadovskiy, D.; Rulyova, N.; Filippov, L. Column flotation of fine glass beads enhanced by their prior heteroaggregation with microbubbles. *Colloids Surf. A Physicochem. Eng. Asp.* **2021**, *617*, 126398. [[CrossRef](#)]
35. Farrokhpay, S.; Filippova, I.; Filippov, L.; Picarra, A.; Rulyov, N.; Fornasiero, D. Flotation of fine particles in the presence of combined microbubbles and conventional bubbles. *Miner. Eng.* **2020**, *155*, 106439. [[CrossRef](#)]
36. Gao, Y.; Dashliborun, A.M.; Zhou, J.Z.; Zhang, X. Formation and stability of cavitation microbubbles in process water from the oilsands industry. *Ind. Eng. Chem. Res.* **2021**, *60*, 3198–3209. [[CrossRef](#)]
37. Shi, H.; Li, M.; Liu, Q.; Nikrityuk, P. Experimental and numerical study of cavitating particulate flows in a venturi tube. *Chem. Eng. Sci.* **2020**, *219*, 115598. [[CrossRef](#)]
38. Li, M.; Bussonnière, A.; Bronson, M.; Xu, Z.; Liu, Q. Study of Venturi tube geometry on the hydrodynamic cavitation for the generation of microbubbles. *Miner. Eng.* **2019**, *132*, 268–274. [[CrossRef](#)]
39. Soyama, H.; Hoshino, J. Enhancing the aggressive intensity of hydrodynamic cavitation through a Venturi tube by increasing the pressure in the region where the bubbles collapse. *Aip Adv.* **2016**, *6*, 045113. [[CrossRef](#)]

40. Bu, X.; Zhou, S.; Tian, X.; Ni, C.; Nazari, S.; Alheshibri, M. Effect of aging time, airflow rate, and nonionic surfactants on the surface tension of bulk nanobubbles water. *J. Mol. Liq.* **2022**, *359*, 119274. [[CrossRef](#)]
41. Pourkarimi, Z.; Rezai, B.; Noaparast, N. Effective parameters on generation of nanobubbles by cavitation method for froth flotation applications. *Physicochem. Probl. Miner. Process.* **2017**, *53*, 920–942.
42. Xiao, W.; Zhao, Y.; Yang, J.; Ren, Y.; Yang, W.; Huang, X.; Zhang, L. Effect of sodium oleate on the adsorption morphology and mechanism of nanobubbles on the mica surface. *Langmuir* **2019**, *35*, 9239–9245.
43. Zhou, S.; Bu, X.; Alheshibri, M.; Zhan, H.; Xie, G. Flocculation structure and dewatering performance of kaolin treated with cationic polyacrylamide degraded by hydrodynamic cavitation. *Chem. Eng. Commun.* **2021**, *209*, 798–807. [[CrossRef](#)]
44. Wang, X.; Zhou, S.; Bu, X.; Ni, C.; Xie, G.Y.; Peng, Y.L. Investigation on interaction behavior between coarse and fine particles in the coal flotation using focused beam reflectance measurement (FBRM) and particle video microscope (PVM). *Sep. Sci. Technol.* **2020**, *56*, 1418–1430. [[CrossRef](#)]
45. Nazari, S.; Ziaedin Shafaei, S.; Hassanzadeh, A.; Azizi, A.; Gharabaghi, M.; Ahmadi, R.; Shahbazi, B. Study of effective parameters on generating submicron (nano)-bubbles using the hydrodynamic cavitation. *Physicochem. Probl. Miner. Process.* **2020**, *56*, 884–904. [[CrossRef](#)]
46. Alheshibri, M.; Qian, J.; Jehannin, M.; Craig, V.S. A history of nanobubbles. *Langmuir* **2016**, *32*, 11086–11100. [[CrossRef](#)] [[PubMed](#)]
47. Bu, X.; Alheshibri, M. The effect of ultrasound on bulk and surface nanobubbles: A review of the current status. *Ultrason. Sonochem.* **2021**, *76*, 105629. [[CrossRef](#)]
48. Hassanzadeh, A.; Hassas, B.V.; Kouachi, S.; Brabcova, Z.; Celik, M.S. Effect of bubble size and velocity on collision efficiency in chalcopyrite flotation. *Colloids Surf. A Physicochem. Eng. Asp.* **2016**, *498*, 258–267. [[CrossRef](#)]
49. Gungoren, C.; Ozdemir, O.; Ozkan, S.G. Effects of temperature during ultrasonic conditioning in quartz-amine flotation. *Physicochem. Probl. Miner. Process.* **2017**, *53*, 687–698.
50. Yoon, R.; Luttrell, G. The effect of bubble size on fine particle flotation. *Miner. Process. Extr. Metall. Rev.* **1989**, *5*, 101–122. [[CrossRef](#)]
51. Xu, M.; Vanderbruggen, A.; Kupka, N.; Zhang, H.; Rudolph, M. Influence of MIBC on the surface-air nucleation and bubble-particle loading in graphite froth flotation. *Miner. Eng.* **2022**, *185*, 107714. [[CrossRef](#)]
52. Li, C.; Zhang, H. A review of bulk nanobubbles and their roles in flotation of fine particles. *Powder Technol.* **2022**, *395*, 618–633. [[CrossRef](#)]